Vol. 206: 59–71, 2000 | MARINE ECOLOGY PROGRESS SERIES
Mar Ecol Prog Ser | Published November 3

Benthic carbon mineralization in a high-Arctic sound (Young Sound, NE Greenland)

Ronnie Nøhr Glud[1,*], Nils Risgaard-Petersen[2], Bo Thamdrup[3], Henrik Fossing[2], Søren Rysgaard[2]

[1]Marine Biological Laboratory, Copenhagen University, Strandpromenaden 5, 3000 Helsingør, Denmark
[2]National Environmental Research Institution, Department of Lake and Estuarine Ecology, Vejlsøvej 25, 8600 Silkeborg, Denmark
[3]Danish Center for Earth System Science, Institute of Biology, Odense University, Campusvej 55, 5230 Odense M, Denmark

ABSTRACT: Benthic carbon mineralization was investigated along a depth transect across a sound in the high Arctic. Aerobic mineralization accounted for approximately 30% of the total degradation. Anaerobic degradation, responsible for the remaining 70%, was dominated by sulfate- and iron respiration, while denitrification and manganese respiration were of marginal importance. The total benthic degradation rate exhibited a rapidly attenuating exponential decline with increasing water depth. Permanent carbon burial accounted for approximately 50% of the total degradation rate, and was comparable to estimates from similar settings at lower latitudes. At the shallow stations, benthic infauna stimulated the benthic oxygen exchange by a factor of 1.5 to 3 relative to molecular diffusion. However, the estimated metabolic activity of the fauna itself accounted for <10% of total benthic degradation. From the rates of benthic degradation, permanent burial, pelagic primary production, and sedimentation of organic carbon, a budget for the pelagic-benthic coupling for outer Young Sound was established. Pelagic production accounted for only a minor fraction of the carbon required by the benthic community, and $\delta^{13}C$ values suggested that terrestric carbon inputs were significant. However, the budget also indicated that additional sources of labile organic carbon (ice-algae, benthic microphytes and oceanic inputs) were important. During July, the time of the summer bloom, 36% of the sedimenting organic material was either degraded or buried. The remainder fueled the community respiration during the long, non-productive, winter.

KEY WORDS: Sediment · Benthic exchange · Fluxes · Oxygen · Carbon · Burial

INTRODUCTION

The Arctic region is characterized by large inter-seasonal variations in pelagic production. Typically, a distinct bloom is associated with melting of the ice cover, and is followed by smaller summer blooms, depending on hydrographic conditions and nutrient balance (e.g. Wassmann & Slagstad 1993). It is estimated that for coastal environments 25 to 50% of the carbon fixed by the pelagic primary producers reaches the sediment surface (Berger et al. 1989). A significant fraction of this material undergoes oxidation through a complex web of degradation processes, while the remainder is permanently buried (Berner 1980). The sediment thereby acts as a source of nutrients and inorganic carbon for the continued water-column production, as well as acting as a sink in regional and global nutrient and carbon cycles. The important electron acceptors for benthic degradation have been identified as O_2, NO_3^-, Mn(IV), Fe(III) and SO_4^{2-} (e.g. Jørgensen 1982, Canfield et al. 1993, Thamdrup 2000). The relative importance of the various pathways varies between

*E-mail: mblrg@mail.centrum.dk

regions, but it has been shown that for coastal environments sulfate reduction generally accounts for the major fraction of total benthic degradation (Jørgensen 1977, Canfield et al. 1993, Thamdrup & Canfield 1996, Thamdrup et al. 1996, Kostka et al. 1999).

Despite a long period of ice cover and low irradiance in winter, the annual pelagic production is surprisingly high in Arctic regions (Sambrotto et al. 1984, Subbarao & Platt 1984). More recent investigations have presented correspondingly high benthic degradation rates for these areas (Grebmeier & McRoy 1989, Henriksen et al. 1993, Hulth et al. 1994, Rysgaard et al. 1996, Glud et al. 1998, Kostka et al. 1999). A seasonal study of benthic mineralization at a single station in Young Sound, NE Greenland, demonstrated an immediate increase in the benthic degradation rates following the bloom after ice melting (Rysgaard et al. 1998). However, due to rapid mineralization of the labile fraction, respiration rates returned to a lower level within 1 mo, and remained there during the rest of the year (Rysgaard et al. 1998). Although most studies suggest that, qualitatively speaking, biogeochemical cycles in permanently cold, coastal, marine arctic ecosystems function similarly to their temperate counterparts, very few studies that allow quantitative assessment of benthic-pelagic coupling have been presented.

The aim of the present study is to give an integrated estimate of the benthic mineralization and the benthic-pelagic coupling for the whole of outer Young Sound, as representative of the numerous fjord systems along the east coast of Greenland. The present work expands on previous investigations of benthic mineralization that were performed at a single position in Young Sound (Rysgaard et al. 1998). The combined data set is discussed in relation to composition and abundance of benthic macrofauna, measurements of primary production and sedimentation. The study adds to the still limited database on benthic degradation in the High Arctic.

MATERIALS AND METHODS

Study site and sampling. The measuring campaign was carried out in the period 21 to 31 July 1996 at Young Sound, NE Greenland (Rysgaard et al. 1996) (Fig. 1). The sound was ice-covered until mid-July. However, drifting local ice stayed in the sound for another 2 wk before it was exported to the Greenland Sea. During the ice-free period, pack ice often entered the sound until regular sea ice was formed in the beginning of October. The surface area of the outer sound is 131.3 km^2, while the total seafloor area is approximately 0.5% larger due to sediment macrotopography (Fig. 1). The seafloor was mapped by use of a combined GPS/Echo-Sounder, and the area at various depth intervals, is given in Table 1. Off Daneborg, 5 stations, ranging in water depth from 20 to 163 m, were selected as representative of the sediments of outer Young Sound. Bottom water was sampled with a 5 l Niskin-sampler. Geographical positions, water depth, temperature, salinity, and nutrient concentrations of the bottom water are given in Table 2. The water column was stratified by a halocline at a water depth around 15 m (not shown), and the most shallow stations showed slightly lower salinity than the deeper stations (Table 2). While the O_2 concentration at all stations was very close to saturation, the nutrient concentrations (NO_3^-, NH_4^+, Si) generally rose with increasing water depth (Table 2). No change in bottom-water characteristics was observed during the sampling period.

Sediment cores were collected in Plexiglas tubes (i.d. 5.3 cm, length 30 cm) using a modified 'Kajak-sampler' (KC-Denmark, Silkeborg). Cores for benthic-exchange measurements were collected during the first 2 d of the measuring campaign. All cores were placed in dark, insulated boxes and brought back to the laboratory within 2 h after sampling. In the laboratory, sediment cores were placed in an incubation tank filled with bottom-water kept at *in situ* temperature. The water was flushed with air to maintain air-saturation. Rotation of small Teflon-coated magnets, attached to the inner wall of each coreliner, ensured a well-mixed overlying water phase inside the tubes (Rasmussen & Jørgensen 1992).

Oxygen microprofiles. A total of 9 O_2 microprofiles was measured in 3 different sediment cores from each station using Clark-type microelectrodes equipped with a guard cathode and an internal reference (Revsbech 1989). The microelectrodes had tip diameters of 5 to 20 µm, the stirring effect was <1%, and the 90% response time was <1 s (Glud et al. 2000). The sensors were positioned by a motor-driven micromanipulator and the sensor current was measured with a picoammeter connected to an A/D converter that transferred the signals to a PC (Revsbech & Jørgensen 1986). Profiles were only measured at sites that were visually unaffected by faunal activity and at a depth resolution of 200 µm. No significant difference was observed between profiles obtained in different cores from a given station (data not shown).

The diffusive O_2 uptake (DOU) was calculated from the concentration gradients measured within the diffusive boundary layer (DBL) by $DOU = -D_0 \delta C/\delta Z$, where D_0 is the molecular diffusion coefficient and C the O_2 concentration at depth Z (Crank 1983). The diffusion coefficient was from Broecker & Peng (1974) and was corrected for temperature as described by Li & Gregory (1974). The depth distribution of the diffusive-

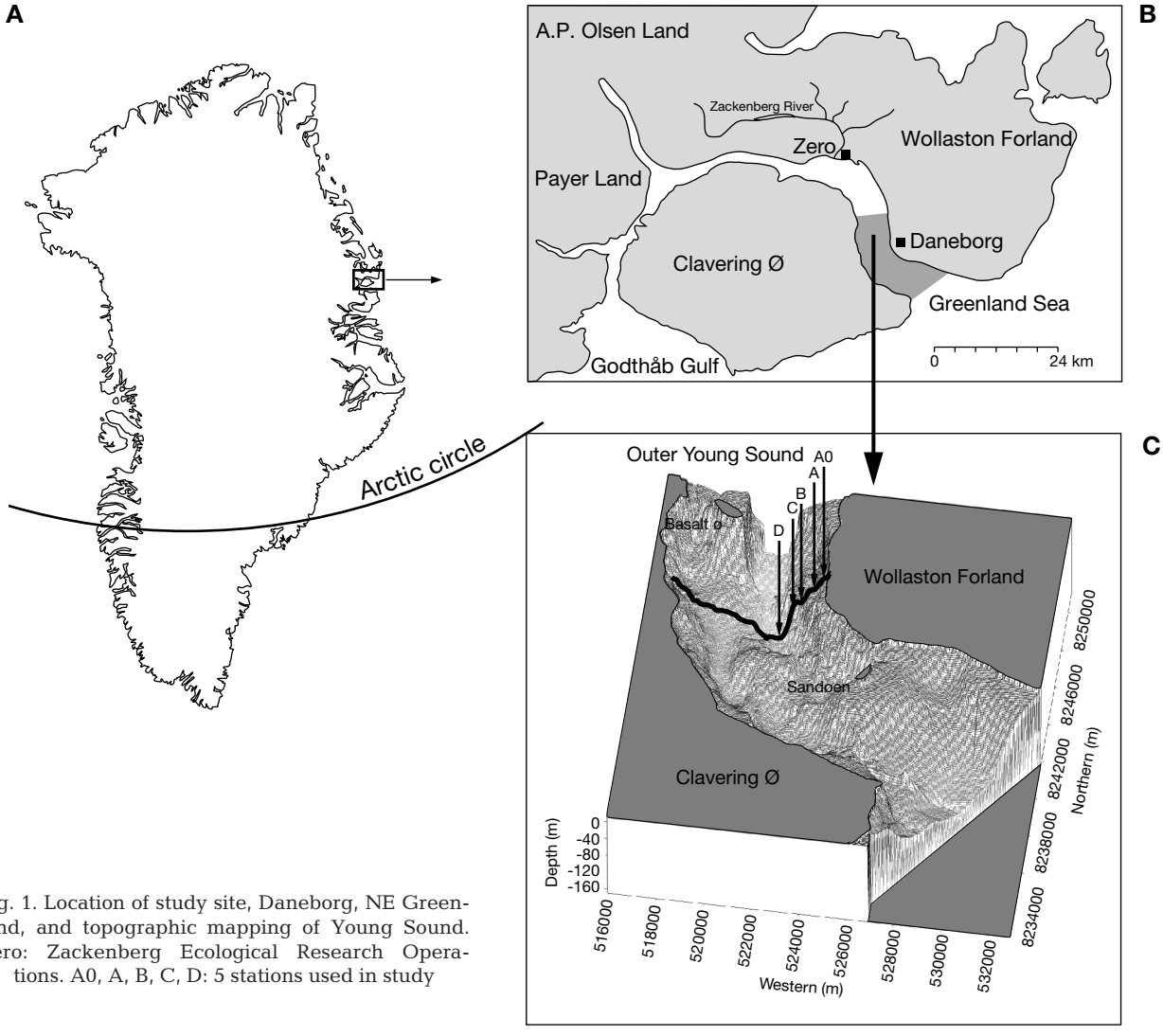

Fig. 1. Location of study site, Daneborg, NE Greenland, and topographic mapping of Young Sound. Zero: Zackenberg Ecological Research Operations. A0, A, B, C, D: 5 stations used in study

based specific O_2 respiration was calculated using the numerical routine of Berg et al. (1998). The sediment diffusion coefficient (D_s) for O_2 was derived from the molecular diffusion coefficient corrected for tortuosity by $D_s = D_0 \phi^2$, where ϕ is the porosity (Ullmann & Aller 1982).

Solute exchange rates. Total exchange rates of O_2 (TOU), dissolved inorganic carbon (DIC), NH_4^+, NO_3^-, PO_4^{3-} and Si were measured by whole-core incubation. After O_2 microprofile measurements, 6 sediment cores from each station were capped, leaving an internal water height of approx. 10 cm. After an incubation period of 6 to 36 h, water samples (25 ml) were collected from each core. Cores were incubated in the dark, and the O_2 concentration was never allowed to decrease by more than 30%. The samples were collected with glass syringes and divided into 3 fractions for O_2, DIC, and nutrient analysis, respectively. For O_2 and DIC measurements, the collected water was transferred to 7 ml gas-tight glass vials. Oxygen concentrations were determined by Winkler titration (Strickland & Parsons 1972), while DIC samples were preserved with 100 µl saturated $HgCl_2$ solution for later analysis on a coulometer (CM5012, UIC. Joliet, Illinois, USA). Samples for nutrient analysis were frozen (–18°C) in plastic vials. Nitrate was determined using standard techniques (Grasshoff et al. 1983) on a flow-injection analyzer (Perstop Analytical, Wilsonville, Oregon, USA), while NH_4^+ was analyzed colorimetrically as described by Bower & Holm-Hansen (1980). Urea concentrations were analyzed using the diacetylmonoxime method as described by Price & Harrison (1987). Phosphate and Si concentrations were determined by standard colorimetric methods as described by Grasshoff et al. (1983). Total exchange rates were calculated from the change in solute concentration during incubation, accounting

Table 1. Seafloor area at given water-depth intervals in Young Sound, Greenland

Water depth interval (m)	Seafloor area (km^2)
0–10	20.3
10–20	8.8
20–30	6.8
30–40	6.1
40–50	6.6
50–60	7.4
60–70	10.1
70–80	10.8
80–90	12.9
90–100	12.5
100–110	9.6
110–120	7.8
120–130	5.1
130–140	1.6
140–150	1.8
150–160	2.1
160–170	1.4
170–180	0.1
Total area	131.8

for the incubation time and the water height above the sediment surface. All sediment uptake rates are defined as negative fluxes (negative sign) while sediment release rates are defined as positive.

We also attempted to measure the total benthic exchange rate of O_2 and DIC *in situ* using the benthic lander ELINOR (Glud et al. 1995). However, due to drifting ice that trapped the surface buoy, and a stony bottom that hindered chamber insertion, most deployments failed. Only 1 successful deployment was achieved. The solute analyses and flux calculation were performed as in the laboratory incubations.

Denitrification. Following the core incubation and a re-equilibration period of approximately 12 h, denitrification was measured in 6 parallel cores applying the isotope-pairing technique (Nielsen 1992, Rysgaard et al. 1995). $^{15}NO_3^-$ was added to a final concentration of approximately 40 µM to the ambient water (the calculated denitrification rate is not affected by the tracer concentration above a certain threshold; e.g. Nielsen & Glud 1996. Cores were then preincubated for 24 h to ensure a steady-state $^{15}NO_3^-$ profile, and cores were subsequently processed individually at 4 h intervals. Production of labeled N_2 was determined from the linear increase over time. Samples for ^{15}N abundance in NO_3^- were frozen while samples for ^{15}N-N_2 were preserved in gas-tight glass vials spiked with a 2% $ZnCl_2$ solution (50% W/W). The relative abundance of $^{14}N^{15}N$ and $^{15}N^{15}N$ was analyzed on a gas chromatograph coupled to a triple-collector isotopic-ratio mass spectrometer (Robo-Prep G+ in line with TracerMass, Europa Scientific, Crewe, UK) as described by Risgaard-Petersen & Rysgaard (1995). The ^{15}N isotopic fraction in the NO_3^- pool was analyzed after reduction of NO_3^- to N_2 using a pure culture of denitrifying bacteria (Risgaard-Petersen et al. 1993). Denitrification rates were calculated from the relative fraction of labeled and unlabeled N_2 and NO_3^-, and the absolute concentration of NO_3^- (Nielsen 1992).

Sediment characteristics, accumulation and burial. Sediment porosity was determined from density and water content measured as the weight loss after drying at 105°C for 24 h. The measurements were performed in 4 parallel cores at a resolution of 0.3 to 1.0 cm. For organic carbon and total N analysis, 4 sediment cores were sliced into similar sections. Each fraction was acidified (HCl) and freeze-dried prior to measurements on an elemental analyzer (RoboPreb-C/N, Europa Scientific, Crewe, UK). For determination of the sediment burial rate, 4 cores from each of Stns A and C were sectioned into 0.5 to 1.0 cm fractions down to a depth of 12 cm. The fractions were freeze-dried and homogenized prior to analysis of the ^{210}Pb and ^{137}Cs content (Joshi 1987). Sediment accumulation was calculated as described by Christensen (1982), while carbon burial rates were calculated from the ^{210}Pb data, density, dry weight and average carbon content at a sediment depth of 11 cm. The stone-content (diam. >10 mm) of the surface sediment (upper 5 cm) was determined by sieving a total of 10 van Veen grab samples per station, each covering an area of 400 cm^2. The various sediment characteristics are given in Table 3.

Table 2. Stations, geographical positions, water depth, oxygen concentrations, nutrient concentrations, salinity and temperature of bottom water. %sat: % saturation

Stn	Positions (latitude, longitude)	Water depth (m)	Temperature (°C)	O_2 (µM, % sat)	S (psu)	NO_3^- (µM)	NH_4^+ (µM)	Si (µM)
A0	74°18′58″, 20°14′48″	20	–0.9	358 (96%)	31.8	1.1	0.5	2.6
A	74°18′58″, 20°15′04″	36	–1.3	363 (96%)	32.2	3.2	0.6	6.5
B	74°18′58″, 20°15′74″	60	–1.3	360 (96%)	33.0	5.4	0.6	7.2
C	74°18′58″, 20°16′92″	85	–1.3	363 (97%)	33.0	6.0	0.7	8.3
D	74°18′58″, 20°18′00″	163	–1.3	362 (96%)	33.0	5.9	1.0	17.4

Table 3. Organic carbon content, C/N-ratio, porosity, and density of surficial sediment, stone content (diam. >10 mm) of the upper 5 cm of sediment, sediment accumulation, and carbon burial rate, calculated as described in 'Materials and methods'

Stn	Organic C (%)	C/N (atomic ratio)	Porosity (v/v)	Density (g cm^{-3})	Stone-content (v/v)	Accumulation (cm yr^{-1})	C-burial rate (mmol C m^{-2} yr^{-1})
A0	0.6	12.2	0.46	1.69	0.169	–	–
A	1.4	10.3	0.65	1.44	0.128	0.23	2110
B	1.1	11.8	0.62	1.52	0.022	–	–
C	1.1	11.4	0.67	1.45	0.017	–	–
D	1.2	11.6	0.75	1.36	0.001	0.14	971

The $\delta^{13}C$ content of the organic material was analyzed for filtered sediment-trap samples, suspended matter from the Zackenberg river collected on filtres, and for homogenized sediment samples from Stn A. Prior to analysis, the samples were treated with HCl, freeze-dried, homogenized, and weighed into sample boats. Samples were combusted in a Robo-Prep elemental analyzer interfaced with a Europa Scientific continuous-flow stable-isotope mass spectrometer. Two reference standards were run for every 5 unknowns, and on the basis of replicate measurements of standard material (Europa Scientific, UK), we estimate our analytical precision to be ±0.3 per mil. All stable-isotope values are reported in δ notation relative to the Pee Dee Belmnite standard: $\delta^{13}C = 1000 \times \{[(^{13}C_{unk}/^{12}C_{unk}) \div (^{13}C_{std}/^{12}C_{std})] - 1\}$.

Sulfate reduction. At each station, 2 undisturbed sediment cores were injected at 1 cm intervals (from 0.5 to 9.5 cm depth) with approximately 5 µl of 80 kBq ml^{-1} $^{35}SO_4^{2-}$ carrier-free tracer (Risø, Denmark) using the whole-core $^{35}SO_4^{2-}$ method developed by Jørgensen (1978). Overlying water was removed to allow a natural oxygen penetration to the surface sediment, and the cores were incubated for 24 h in the dark at temperatures reflecting *in situ* conditions. Following incubation, the bacterial activity was stopped by slicing the cores at 1 cm intervals and pooling equal intervals into an equivalent volume of 20% zinc-acetate-solution (w/v). The sediment samples were then frozen (–18°C) for later analysis. Bacterial sulfate reduction rates were quantified from the reduction of $^{35}SO_4^{2-}$ into total reducible inorganic sulfur (TRIS = $H_2{}^{35}S$, $Fe^{35}S$, $Fe^{35}S_2$, and $^{35}S^o$) and determined using the 1-step acidic Cr-II method (Fossing & Jørgensen 1989). A Canberra-Packard 2400 TR liquid-scintillation counter (with Packard Ultima Gold XR scintillation fluid) was used to determine the $Zn^{35}S$ and $^{35}SO_4^{2-}$ radioactivity.

The sulfate reduction rate (SRR) was calculated from the fraction of reduced sulfur produced during incubation and the *in situ* sulfate concentration,

$$SRR = \frac{a}{A+a} \cdot [SO_4^{2-}] \cdot \frac{1}{d} \cdot 1.06 \text{ nmol cm}^{-3} \text{ d}^{-1} \quad (1)$$

where a is the radioactivity of the reduced sulfur compounds per volume sediment, A the radioactivity of the sulfate per volume sediment after incubation, $[SO_4^{2-}]$ the sulfate concentration (nmol cm^{-3}), d the incubation time in days, and 1.06 the isotopic fractionation factor (Jørgensen & Fenchel 1974).

Sulfate concentrations were determined on 100-fold diluted and filtered pore water samples by non-suppressed anion-exchange chromatography (Waters 510 HPLC Pump; Waters IC-Pak 50 × 4.6 mm anion-exchange column; and Waters 430 Conductivity Detector). Isophtalic acid (1 mM) in 10% methanol (pH 4.6) was used as eluent.

Total carbon and nitrogen mineralization rates (bag incubations). At 2 stations (A and C), the depth distribution of carbon and nitrogen mineralization was determined using anoxic incubation in gas-tight plastic bags (Canfield et al. 1993, Hansen et al. 2000). From 16 sediment cores, sampled in parallel to the measurements described above, the upper 10 cm were sectioned in 8 depth intervals in an N_2-filled glove bag. Sediment from the same depth horizon in the parellel cores was pooled, homogenized and transferred into gas-tight, laminated plastic bags (Hansen et al. 2000). The bags were incubated at *in situ* temperature in larger N_2-filled bags for a total of 15 d. During this period, 5 subsamples were recovered and porewater was extracted through 0.45 µm cellulose-acetate filters by pneumatic squeezing in an N_2-filled glove bag. Samples for DIC and NH_4^+ were analyzed using a flow injection-conductivity detection system (Hall & Aller 1992). In parallel, samples for dissolved Fe^{2+} and Mn^{2+} were recovered and acidified for later analysis. Concentrations of dissolved Fe^{2+} were determined by colorimetry with a Ferrozine solution (Stookey 1970), while dissolved Mn^{2+} was determined by flame atomic-absorption spectroscopy. The initial concentrations of available manganese oxides and poorly crystalline iron oxides in the homogenized sediments were determined in samples collected under an N_2 atmosphere, by means of dithionite and oxalate extractions, respectively (Thamdrup & Canfield 1996). Total organic carbon mineralization rates and porewater accumulation rates of

NH_4^+, Mn^{2+}, and Fe^{2+} were calculated from the linear increases in concentrations (Canfield et al. 1993).

SRR of the homogenized sediment were determined by injection of $^{35}SO_4^{2-}$ into subsamples of sediment followed by 24 h anoxic incubation, with analysis and calculations as described above. The organic carbon mineralization coupled to sulfate reduction was calculated assuming a reaction stoichiometry of SO_4^{2-} to organic carbon of 1:2 (Canfield et al. 1993). The sulfate-independent carbon oxidation was calculated by subtracting the sulfate-dependent mineralization from the total accumulation of DIC in each depth interval. In the sediment below the O_2- and NO_3^--containing surface layer, the difference was ascribed to bacterial reduction of either iron or manganese depending on the depth distribution of manganese and iron oxide and the accumulation rate of Fe^{2+} and Mn^{2+} in the bag incubations (Thamdrup & Canfield 1996). The stoichiometry of NO_3^- reduction to organic carbon oxidation was assumed to be 4:5 (Canfield et al. 1993).

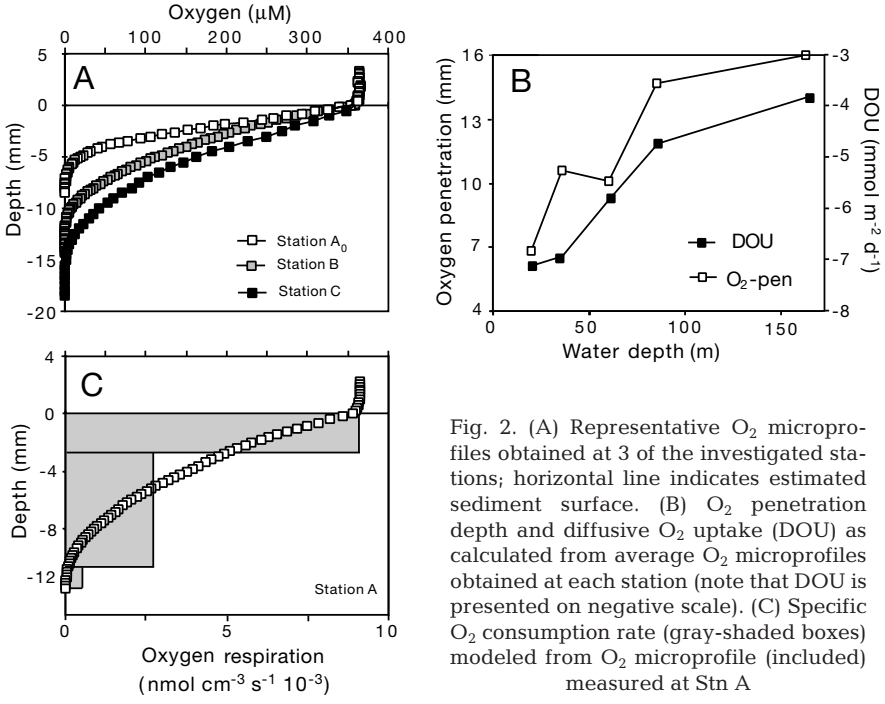

Fig. 2. (A) Representative O_2 microprofiles obtained at 3 of the investigated stations; horizontal line indicates estimated sediment surface. (B) O_2 penetration depth and diffusive O_2 uptake (DOU) as calculated from average O_2 microprofiles obtained at each station (note that DOU is presented on negative scale). (C) Specific O_2 consumption rate (gray-shaded boxes) modeled from O_2 microprofile (included) measured at Stn A

RESULTS

O_2 microgradients

Oxygen microprofiles were measured at all 5 stations, and showed a gradual increase in the O_2 penetration depth from 6.8 mm at Stn A0 to a maximum of 16 mm at Stn D (Fig. 2A,B). The diffusive oxygen uptake (DOU) as calculated from the microprofiles also reflected a reduced activity with increasing water depth (Fig. 2B), with a gradual decrease of 3.5 mmol O_2 m^{-2} d^{-1} from Stn A0 to the deep site of Stn D. The specific O_2 consumption showed maximum values at the sediment surface, indicating a recent deposition of labile organic material (Fig. 2C).

Total exchange rates

The total O_2 uptake (TOU) had a maximum of –20.3 ± 4.6 mmol m^{-2} d^{-1} at the most shallow station (A0), and exhibited a strong attenuation with water depth (Fig. 3A). At depths greater than 60 m, the TOU reached a constant value around –3.6 mmol m^{-2} d^{-1} (Fig. 3A). At the deepest stations, DOU was equal to TOU. However, at the 2 most shallow stations TOU exceeded DOU by 3- and 1.5-fold, respectively. The total release rate of DIC mirrored the TOU, and the molar ratio between the O_2 and DIC exchange was close to 1 at all stations (Fig. 3A). The DIC release rate and the TOU could both be described by an exponential decline with increasing water depth (z, in meters) given by DIC-release = 3.25 + 3.53 $e^{(-0.0694Z)}$; TOU = –2.26 – 18.2 $e^{(-0.0525Z)}$ (Fig. 3A). At Stn A, the *in situ* TOU and DIC release rates were not different from the values obtained in the laboratory (Fig. 3A). The release rates of NH_4^+ and PO_4^{3-} were also at a maximum at the most shallow stations and reached constant low values at water depths from 60 m and downwards (Fig. 3B). At the 2 shallowest stations, NO_3^- was taken up by the sediment, while the 3 deeper stations all showed a moderate NO_3^- release (Fig. 3C). The total release rate of N (ΣNH_4^+, NO_3^-, NO_2^-, urea) showed a gradual decrease with increasing water depth, reaching a minimum of 0.02 mmol m^{-2} d^{-1} at the deepest site (Fig. 3C). The silicate flux at Stn A0 was 4.6 ± 0.9 mmol m^{-2} d^{-1}, but only around 0.9 ± 0.1 mmol m^{-2} d^{-1} at the other deeper stations (Fig. 3D).

SRR and denitrification

At all stations, SRR was suppressed near the sediment surface, but increased to a maximum at approxi-

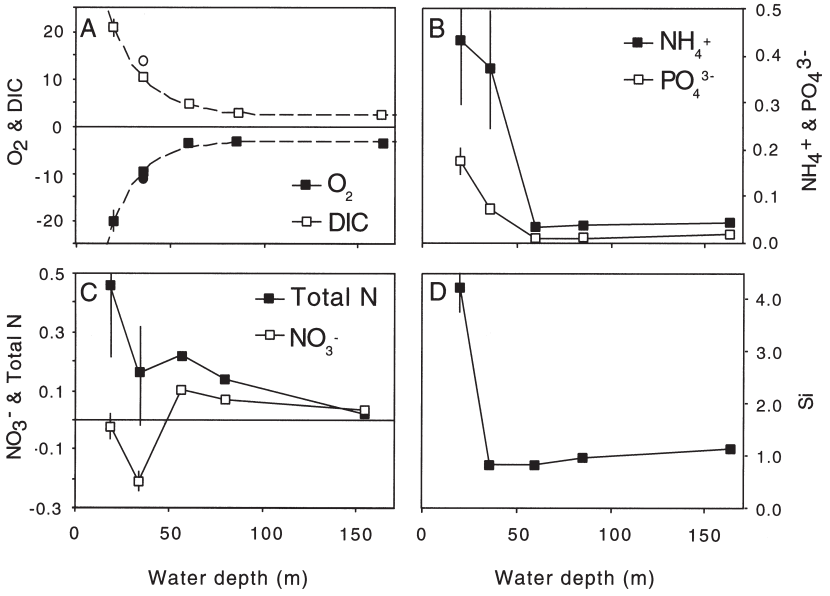

Fig. 3. Total exchange rates (mmol m^{-2} d^{-1}) of dissolved inorganic carbon (DIC), O_2, NH_4^+, PO_4^{3-}, total nitrogen, NO_3^- and Si as a function of water depth. Negative values indicate benthic uptake. In (A), dashed lines indicate best fitted exponential decline with water depth. Standard deviations are shown except when smaller than the symbols). Circles in (A) indicate data obtained *in situ* by a benthic lander (see 'Materials and methods')

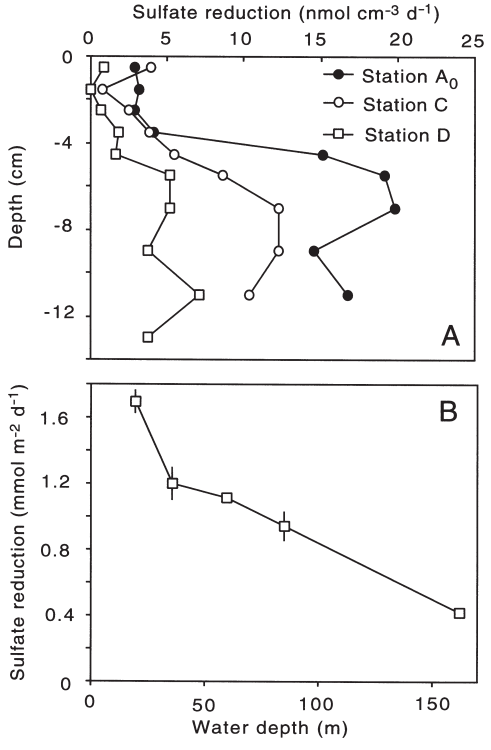

Fig. 4. (A) Selected sulfate reduction rate profiles at 3 of investigated stations. (B) Depth-integrated sulfate reduction rate as a function of water depth. Standard deviations are shown except when smaller than the symbols

mately 6 cm depth (Fig. 4A). The suppressed SRR in the upper 6 cm of the sediment indicates that carbon oxidation in the upper suboxic sediment strata was coupled to nitrate, manganese or iron reduction. As indicated by the depth profiles in Fig. 4A, the depth-integrated SRR (SRR_d) decreased with increasing water depth, from a maximum rate of 1.7 ± 0.1 mmol m^{-2} d^{-1} at Stn A0 to 0.4 ± 0.1 mmol m^{-2} d^{-1} at Stn D (Fig. 4B). However, the attenuation was not as steep as that of the exchange measurements. The relative importance of SRR in oxidation of organic carbon was calculated as (2 · SRR_d/total DIC release) · 100, and equaled 16, 25, 46, 60 and 46% at the 5 stations (listed in order of increasing water depth). These values must represent minima, since SRR was integrated only to a sediment depth of 12 cm.

Denitrification at Stns A and C equaled 0.48 ± 0.1 mmol N m^{-2} d^{-1} and 0.11 ± 0.01 mmol N m^{-2} d^{-1}, respectively. At both stations the amount of N that was denitrified was similar to the total N efflux and accounted for 5 and 3% of the total carbon mineralization quantified as the total DIC release rate, respectively. Including dinitrogen, the C/N ratio of the effluxing inorganic solutes was 15 and 12 at Stns A and C, respectively.

Rates and pathways of anaerobic carbon mineralization (bag-incubations)

Bag-incubations were performed at Stns A and C only. At both stations, DIC and NH_4^+ accumulations exhibited maximum values close to the sediment surface and gradually decreased with increasing depth (Fig. 5). Due to adsorption of NH_4^+ to sediment particles (Rosenfeld 1979), the accumulation rates must represent minimum values. Assuming an adsorption coefficient of 1.3 (Mackin & Aller 1984), the C:N mineralization ratio was equal to 13 and 9 at Stns A and C, respectively. This is somewhat lower than the C:N ratio of the solutes released during the core incubations.

The SRR measured during the bag incubations was repressed at the surface, and first reached maximum at a sediment depth of 5 cm (Fig. 6). Consequently, there was a large divergence of total carbon mineralization rates and carbon mineralization coupled to SRR near the sediment surface. The excess carbon mineralization rates tapered off with depth, and SRR accounted for all mineralization below 8 cm depth. The sediment

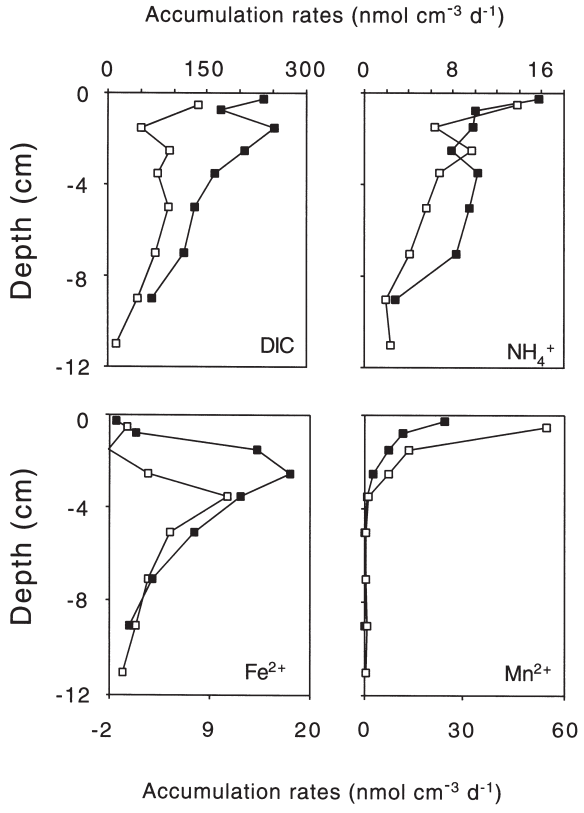

Fig. 5. Accumulation rate of dissolved inorganic carbon (DIC), NH_4^+, Mn^{2+}, Fe^{2+} as a function of sediment depth as quantified by bag-incubation technique. (■) Measurements at Stn A (data have partly been presented in Rysgaard et al. 1998); (□) measurements at Stn C

strata that separated the oxic zone from the zone dominated by SRR (Figs. 2 & 5) showed the highest accumulation rates of soluble Mn^{2+} and Fe^{2+} (Fig. 5). Furthermore, reactive manganese oxides were extracted from 0 to 1.5 cm, while poorly crystalline Fe oxides persisted until a depth of 8 cm (data not shown). These observations suggested that besides denitrification, Mn and/or Fe reduction could contribute significantly to carbon oxidation in these strata. There was no sharp depth separation between the anaerobic mineralization processes, however. To estimate the importance of manganese, iron and sulfate reduction to anaerobic degradation we followed the principles described by Thamdrup & Canfield (1996).

At Stns A and C, the depth-integrated DIC accumulation in the anoxic sediment strata (1 to 10 cm) equaled 12.4 and 6.1 mmol m^{-2} d^{-1}, and SRR in the same depth interval was 2.9 and 2.2 mmol m^{-2} d^{-1}, respectively. With a reaction stoichiometry of 1:2 between SO_4^{2-} and organic carbon, SRR accounted for 47 and 72% of the total anaerobic degradation at Stns A and C, respectively. Using the above denitrification values, the fraction of anaerobic degradation that can be ascribed to this pathway equaled 4 and 2%, respectively. The remainder can be ascribed to manganese and iron reduction. However, little reactive manganese was available at sediment depths below 1 cm, while Fe oxides were present and Fe^{2+} accumulated in these sediment strata (Fig. 5). Precise determination of Mn reduction responsible for carbon oxidation is not possible due to low spatial resolution, but it is very likely that almost all manganese reduction in the anoxic sediment could be ascribed to oxidation of Fe^{2+} (Canfield et al. 1993). Consequently we ascribe all sulfate and nitrate independent anoxic carbon oxidation to iron reduction, amounting to 49 and 26% at Stns A and C, respectively (see also 'Discussion).

Sulfate reduction rates measured during bag incubations were approximately 2.5 times higher than the equivalent values obtained in whole-core incubations (Fig. 6). The DIC accumulation rate measured in the bags was approximately 1.7 and 2.3 times higher than the DIC release rates measured by the core incubations at Stns A and C, respectively. These observations suggest that sediment homogenization stimulated the carbon oxidation rate. The lower C:N ratio of inorganic solutes produced within the bags compared to the whole-core incubation may suggest that relatively labile organic carbon was being made available for anaerobic degradation during homogenization. We do not expect, however, that the various anaerobic carbon oxidation pathways were affected differently (Rysgaard et al. 1998).

To quantitatively compare anaerobic and aerobic degradation rates, the DIC efflux of incubated sediment cores was used as an estimate of total benthic degradation. From the SRR measured by whole-core incubation, and the relative partitioning of the anaero-

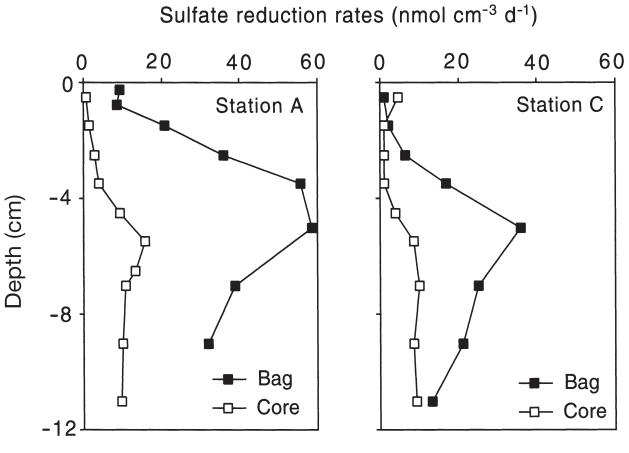

Fig. 6. Sulfate reduction rates as quantified by whole-core incubation technique (□) and by bag-incubation technique (■) at Stns A and C. Bag-incubation data from Stn A have been presented by Rysgaard et al. (1998)

Table 4. Relative importance (%) of various electron acceptors at Stns A and C. Annual integrated values for Stn A have been presented by Rysgaard et al. (1998)

Degradation pathway	Stn A	Stn C
Aerobic	38	20
Denitrification	3	2
Manganese reduction	0	0
Iron reduction	26	21
Sulfate reduction	33	57

bic degradation pathways deduced above, we calculated that aerobic heterotrophic activity accounted for 38 and 20% of the total benthic degradation at Stns A and C, respectively (Table 4). The fraction of TOU not accounted for by aerobic respiration represents the O_2 consumed by reoxidation of reduced inorganic species from anaerobic degradations (62 and 80% at Stns A and C, respectively).

DISCUSSION

Faunal respiration and benthic mineralization

The difference between DOU and TOU has been used as a measure of the benthos-mediated solute exchange (Archer & Devol 1992, Glud et al. 1994). At Stn A0, TOU was approximately 3 times higher than DOU, and this ratio decreased to 1.5 at Stn A, while it was close to 1 at the remaining stations (Figs. 2 & 3). The abundance of macrofauna along the same depth transect attenuated with water depth from a maximum of 2675 individuals m^{-2} at Stn A0 to a minimum of 875 individuals m^{-2} at Stn C (Table 5). The distribution among the trophic groups also changed with depth. The relative abundance of deposit feeders gradually increased from 64% at Stn A0 to 78% at Stn C, while the relative abundance of filter feeders decreased from 17 to 4% (Sejr et al. 2000). The gradual decrease in abundance and the change in trophic composition most likely reflects a decrease in quantity and quality of organic material with increasing water depth (Fig. 3, Table 5). However, at all stations benthic fauna was dominated by deposit-feeding polychaetes, that accounted for 71% of the total population, while bivalves accounted for 10% (Sejr et al. 2000).

From biomass determinations (Sejr et al. 2000) and mass-specific metabolic respiration estimates (Piepenburg et al. 1995), the respiration of the 2 by far dominating faunal groups was estimated (Table 5). At all stations the respiration of polychaetes and bivalves accounted for <10% of TOU. The small fraction of fauna-related O_2 uptake that could be ascribed to faunal metabolism suggests that the elevated difference between TOU and DOU at the fauna-rich stations was caused by enhanced ventilation of the surface sediment. Studies have indicated that fauna-related irrigation, turbation and excretion of labile organic carbon can stimulate benthic microbial activity (Aller 1988, Hansen & Blackburn 1992, Banta et al. 1999). Our calculations suggest that such effects were more important than the metabolic activity of the macrofauna itself for the sequential carbon degradation at shallow water depths in outer Young Sound. Faunal activity, in the form of bioturbation, was also an important factor in determining the relative importance of metals as terminal electron acceptors.

Relative importance of different degradation pathways

The amount of reactive iron oxide was almost 100 times higher than the pool of reactive manganese oxides, and the shallow penetration of Mn-oxides (data not shown) excluded manganese reduction as a significant pathway of degradation of organic carbon in Young Sound (see also Rysgaard et al. 1998). The mod-

Table 5. Total abundance of benthic fauna and relative fraction accounted for by 2 dominant taxa (data from Sejr et al. 2000). Since no information on polychaete biomass was available, we estimated values from relationship between abundance and biomass for 15 species of polychaetes from Disco Fjord (West Greenland) as reported by Schmid & Piepenburg (1993). Respiration was estimated using following mass-specific metabolic rates (µmol O_2 g^{-1} h^{-1}): polychaetes 0.60, bivalves 0.15 (Piepenburg et al. 1995). TOU: total O_2 uptake; –:not determined

Stn	Fauna abundance (individuals m^{-2})	Polychaetes (%)	Polychaetes ($g\ m^{-2}$)	Bivalves (%)	Bivalves ($g\ m^{-2}$)	Respiration (mmol O_2 m^{-2} d^{-1})	Respiration of TOU (%)
A0	2675	70	13.0	10	150	0.73	4
A	1125	78	6.1	12	230	0.92	9
B	1075	78	5.8	11	70	0.34	9
C	875	80	4.8	8	51	0.25	7
D	–	–		–		–	–

est manganese reduction encountered was probably coupled mainly to reoxidation of reduced iron and sulfur, as has been observed in other studies (Canfield et al. 1993, Aller 1994, Kostka et al. 1999). Iron reduction, however, was a quantitatively important degradation pathway. Significant iron reduction requires an efficient countercurrent exchange of reduced and oxidized iron, and intense bioturbation is therefore essential. The high density of deposit-feeding macrofauna seems to ensure sufficient sediment mixing in the permanently cold sediments of Young Sound. At Stn C the most important electron acceptor was sulfate, while nitrate and manganese were of marginal importance. The importance of aerobic degradation at Stn A, however, was relatively high (see references below). This may be related to the high faunal activity at this station combined with the very high O_2 content of the cold bottom-water (Table 2), which also gave rise to the relatively deep O_2 penetration for a so active site.

The still limited database on the relative importance of different benthic degradation pathways indicates that carbon oxidation processes in permanently cold sediments (Rysgaard et al. 1998, Kostka et al. 1999, present study) are not different from those in temperate or tropical sediments (Canfield et al. 1993, Jørgensen 1996, Thamdrup & Canfield 1996, Thamdrup et al. 1996). The same applies to total benthic degradation rates, and the present study aligns with previous measurements performed at comparable water depths (Pfannkuche & Thiel 1987, Grebmeier & McRoy 1989, Henriksen et al. 1993, Hulth et al. 1994, Glud et al. 1998 and references therein).

Pelagic-benthic coupling of outer Young Sound

The benthic degradation rate declined exponentially with water depth and reached almost constant values at water depths of more than 60 m (Fig. 3). Similar observations have been made in other regions, but with much slower attenuation (e.g. Jahnke et al. 1990, Archer & Devol 1992, Hulth et al. 1994, Glud et al. 1999). The sharp attenuation in Young Sound indicates an efficient recycling of organic carbon and nutrients in the upper water column of outer Young Sound.

In July, the zooplankton community, consisting mainly of copepods, very efficiently grazed on the primary producers in the upper 30 to 40 m of the water column (Rysgaard et al. 1999). From biomass determinations it was estimated that 85 to 104% of annual primary production was grazed by copepods. Consequently, organic material produced by pelagic primary producers in the upper 40 m probably left the photic zone as rapidly sinking fecal pellets. The scenario would result in an almost depth-independent carbon input to the deeper parts of the sound, and match our observation of strongly attenuating benthic DIC release rates in the upper 60 m.

Parallel sediment-traps were placed at water depths of 18, 22 and 26 m at the position of Stn A (water depth 36 m). The material collected by the traps was constant with water depth, and the estimated net-sedimentation equaled 2.53 ± 0.19 g dw m^2 d^{-1} (n = 6) for the last half of July. The trap material consisted mainly of unidentifiable amorphous detritus. However, fecal pellets accounted for the largest fraction of collected material that could be identified, and very few algae were indeed encountered. This is in accordance with the high grazing estimates of Rysgaard et al. (1999). Pelagic primary production in July 1996 was quantified as 4.7 g C m^{-2} (524 t C for outer Young Sound) and accounted for 46% of the annual pelagic production (Rysgaard et al. 1999) (Table 6). Applying the fitted exponential decline of the DIC release rates (Fig. 3) and the hypsometry (Table 1), the total benthic inorganic carbon release of outer Young Sound in July equaled 312 t C (Table 6). This is equivalent to 60% of the pelagic primary production measured during the same period.

However, not all organic material reaching the seafloor is mineralized. A fraction of the sedimenting material will be permanently buried in the sediment. The temporal dynamics of burial acts on a longer time scale than mineralization processes, but if we assume for the sake of comparison that the burial rate in Young Sound is constant during the annual cycle, it would equal 5.8 and 2.7 mmol m^{-2} d^{-1} for Stns A and C, respectively (see Table 2). Assuming that sediment burial calculated from Stn D represents sediments at depth > 60 m and that burial at Stn A represents the remaining sediments, then total carbon burial in Young Sound in July equaled 165 t C (Table 6). Both these assumptions are justified by the fact that they were true for the DIC release rates. Thus, the sum of

Table 6. Estimated process throughputs for outer Young Sound in July 1996. Calculations include areas with water depths of 10 to 180 m (see 'Discussion' for details for calculations)

Process	Throughput (t C)
Sources	
Primary production	524
Terrestrial sedimentation	776
Pelagic sedimentation	539
Total sedimentation	1315
Sinks	
Benthic mineralization	312
Permanent burial	165

benthic carbon mineralization and sediment burial accounted for 92% of the pelagic primary production in July. This value is too high, considering pelagic assimilation and mineralization, and suggests alternative sources of organic carbon for the benthic community.

The present study only reflects the conditions in July, and our observations cannot be extrapolated to an annual budget. However, a seasonal study of benthic degradation from Stn A has previously been presented (Rysgaard et al. 1998), in which it was observed that the maximum DIC release rate in July was only 40% higher than measurements obtained during winter. Since primary production exhibits much larger seasonal variation, a temporal dynamic of the benthic degradation at all our stations that is similar to that at Stn A would enhance the imbalance between pelagic production and benthic degradation significantly. Our basin-wide integration suggests that the benthic community of Young Sound has additional carbon sources.

Direct measurements of the sedimentation rate in July quantified the benthic carbon input to 11.8 ± 2.7 g C m^{-2} (n = 6). Using the approach described above, this was equivalent to 1315 ± 300 t C in outer Young Sound, which was significantly more than the pelagic primary production (Table 6). Benthic carbon mineralization and permanent carbon burial in July accounted for 36% of the measured carbon sedimentation. The sediment-trap data thereby indicated a net deposition of carbon during the month of July, of which pelagic production was only a minor fraction. The benthic community could not degrade the sedimentation of July at an equal pace. Thus, the benthic deposition of July to a large extent supported benthic metabolism during the long non-productive winter period. The additional supply of carbon that cannot be ascribed to the pelagic primary producers could potentially be of terrestrial origin. At present no direct measurements elucidating this potential source exist.

However, an estimate can be deduced from the sediment-trap material collected at Stn A in July which had a measured $\delta^{13}C$ value of –24.7 ± 0.3 (n = 10). The corresponding average value for the upper 14 cm of the sediment at the same station was –23.1 ± 0.4 (n = 20). These values are intermediate compared to the values of Arctic pelagic primary producers (–21.6 ± 0.3 [Hobson & Welch 1992]), and to resuspended organic material in the single largest freshwater source to Young Sound (Zackenberg River: see Fig. 1) which was –26.9 ± 0.3 (n = 3). In comparison, ice algae and arctic kelps have $\delta^{13}C$ values around –20.7 ± 0.9 and –20.1 ± 0.4, respectively (Hobson & Welch 1992). Assuming an average $\delta^{13}C$ value of primary producers of –21.6, it can be estimated that 59% of the organic material in the sediment trap at Stn A in July was of terrestrial origin. Extrapolated to the outer Young Sound, this corresponds to benthic inputs of terrestrial and pelagic organic carbon of 776 and 539 t C, respectively (Table 6). It is likely that benthic carbon degradation (and burial) in outer Young Sound is, to a significant extent, founded on terrestrial inputs. The estimate of pelagic input to the trap material (539 t C) accounts for 103% of local pelagic primary production. Since only a minor fraction of the gross primary production ever reaches the sediment, this indicates that other sources of labile organic carbon must be important. The remaining potential sources are ice algae, benthic primary producers, or import from the Greenland Sea. At present no reliable production estimates for these sources exist.

Acknowledgements. This study was financially supported by The Danish Research Council, The Danish Research Foundation, The European Union under the framework MAST III, and the Max Planck Society. The Danish Military Division, Sirius, is gratefully acknowledged for their hospitality and help during the study. Additionally we would like to thank Egon Frandsen, Marlene Skjærbæk, Kitte Gerlich, Anna Haxen, Kirsten Neumann and Ola Holby for technical assistance and help in the field.

LITERATURE CITED

Aller RC (1988) Benthic fauna and biogeochemical processes in marine sediments: the role of burrow structures. In: Blackburn TH, Sørensen J (eds) Nitrogen cycling in marine environments. Wiley & Sons, London, p 301–338

Aller RC (1994) Sedimentary Mn cycle in Long Island Sound: its role as intermediate oxidant and influence of bioturbation, O_2 and C_{org} flux on diagenetic reaction balances. J Mar Res 52:259–295

Archer D, Devol A (1992) Benthic oxygen fluxes on the Washington shelf and slope: a comparison of *in situ* microelectrode and chamber flux measurements. Limnol Oceanogr 37:614–629

Banta GT, Holmer M, Jensen MH, Kristensen E (1999) Effects of two polychaete worms, *Nereis diversicolor* and *Arenicola marina*, on aerobic and anaerobic decomposition in a sandy marine sediment. Aquat Microb Ecol 19:189–204

Berg P, Risgaard-Petersen N, Rysgaard S (1998) Interpretation of measured concentration profiles in sediment pore water. Limnol Oceanogr 43:1500–1510

Berger WH, Smetacek VS, Wefer G (1989) Ocean productivity and paleoproductivity — an overview. In: Berger WH, Smetacek VS, Wefer G (eds) Productivity of the ocean: present and past. John Wiley & Sons, London, p 1–34

Berner RA (1980) Early diagenesis: a theoretical approach. Princeton University Press, Princeton

Bower E, Holm-Hansen HA (1980) A salicylate-hypochlorite method for determining ammonia in seawater. Can J Fish Aquat Sci 37:794–798

Broecker WS, Peng TH (1974) Gas exchange rates between air and sea. Tellus 26:21–35

Canfield DE, Jørgensen BB, Fossing H, Glud RN, Gundersen JK, Thamdrup B, JW Hansen, Nielsen LP, Hall POJ (1993) Pathways of organic carbon oxidation in three continental margin sediments. Mar Geol 113:27–40

Christensen E (1982) A model for radionucleides in sediments influenced by mixing and compaction. J Geophys Res 87: 566–572

Crank J (1983) The mathematics of diffusion. Clarendon Press, Oxford

Fossing H, Jørgensen BB (1989) Measurement of bacterial sulfate reduction in sediments: evaluation of the single-step chromium reduction method. Biogeochemistry 8: 223–245

Glud RN, Gundersen JK, Jørgensen BB, Revsbech NP, Schulz HD (1994) Diffusive and total oxygen uptake of deep-sea sediments in the eastern South Atlantic Ocean: *in situ* and laboratory measurements. Deep-Sea Res 41:1767–1788

Glud RN, Gundersen JK, Revsbech NP, Jørgensen BB, Huettel M (1995) Calibration and performance of the stirred flux chamber from the benthic lander Elinor. Deep-Sea Res 42:1029–1042

Glud RN, Holby O, Hofmann F, Canfield DE (1998) Benthic mineralization in Arctic sediments (Svalbard). Mar Ecol Prog Ser 173:237–251

Glud RN, Gundersen JK, Holby O (1999) Benthic *in situ* respiration in the upwelling area off central Chile. Mar Ecol Prog Ser 186:9–18

Glud RN, Gundersen JK, Ramsing NB (2000) Electrochemical and optical oxygen microsensors for in situ measurements. In: Buffle J, Horvai G (eds) In situ analytical techniques for water and sediment. Wiley, Chichester, p 19–73

Grasshoff K, Erhardt M, Kremling K (1983) Methods of seawater analysis, 2nd edn. Verlag Chemie, Weinheim

Grebmeier JM, McRoy CP (1989) Pelagic-benthic coupling on the shelf of northern Bering and Chukchi Seas. III. Benthic food supply and carbon cycling. Mar Ecol Prog Ser 53: 79–91

Hall POJ, Aller RC (1992) Rapid, small-volume, flow injection analysis for $\sum CO_2$ and NH_4^+ in marine and freshwaters. Limnol Oceanogr 37:1113–1119

Hansen LS, Blackburn TH (1992) Mineralization budgets in sediment micrcosmos: effect of the infauna and anoxic conditions. FEMS Microbiol Ecol 102:33–43

Hansen JW, Thamdrup B, Jørgensen BB (2000) Anoxic incubation of sediment in gas-tight plastic bags: a method for biogeochemical process studies. Mar Ecol Prog Ser (in press)

Henriksen KT, Blackburn H, Lomstein BA, McRoy CP (1993) Rates of nitrification, distribution of nitifying bacteria and inorganic N fluxes in the northern Bering-Chuckchi shelf sediments. Cont Shelf Res 13:629–651

Hobson KA, Welch EW (1992) Determination of trophic relationships within a high Arctic marine food web using $\delta^{13}C$ and $\delta^{15}N$ analysis. Mar Ecol Prog Ser 84:9–18

Hulth S, Blackburn TH, Hall POJ (1994) Arctic sediments (Svalbard): consumption and microdistribution of oxygen. Mar Chem 46:293–316

Jahnke RA, Reimers, CE Craven, DB (1990) Intensification of recycling of organic matter at the sea floor near ocean margins. Nature 348:50–54

Jørgensen BB (1977) The sulfur cycle of a coastal marine sediment (Limfjorden, Denmark. Limnol Oceanogr 5:814–832

Jørgensen BB (1978) A comparison of methods for quantification of bacterial sulfate reduction in coastal marine sediments. 1. Measurement with radiotracer techniques. Geomicrobiol J 1:11–28

Jørgensen BB (1982) Mineralization of organic matter in the sea bed — the role of sulfate reduction. Nature 296: 643–645

Jørgensen BB (1996) Case study — Aarhus bay. In: Jørgensen BB, Richardsen K (eds) Eutrophication in coastal and marine ecosystems. Series IV. American Geophysical Union, Washington DC, p 137–154

Jørgensen BB, Fenchel T (1974) The sulfur cycle of a marine model system. Mar Biol 24:189–201

Joshi SR (1987) Non-destructive determination of lead-210 and radium-226 sediments by direct photon analysis. J Radioanalyt Nucl Chem Art 116:169–182

Kostka JE, Thamdrup B, Glud RN, Canfield DE (1999) Rates and pathways of carbon oxidation in permanently cold Arctic sediments Mar Ecol Prog Ser 180:7–21

Li YH, Gregory S (1974) Diffusion of ions in deep-sea sediments. Geochim Cosmochim Acta 38:703–714

Mackin JE, Aller R (1984) Ammonium adsorption in marine sediments. Limnol Oceanogr 29:250–257

Nielsen LP (1992) Denitrification in sediment determined from nitrogen pairing. FEMS Microb Ecol 86:357–362

Nielsen LP, Glud RN (1996) Denitrification in a coastal sediment measured *in situ* by the nitrogen isotope pairing technique applied to a benthic flux chamber. Mar Ecol Prog Ser 137:181–186

Pfannkuche O, Thiel H (1987) Meiobenthic stocks and benthic activity on the NE-Svalbard Shelf and in the Nansen Basin. Polar Biol 7:253–266

Piepenburg D, Blackburn TH, von Dorrien CF, Gutt J, Hall POJ, Hulth S, Kendall MA, Opalinski KW, Rachor E, Schmid MK (1995) Partitioning of benthic community respiration in the Arctic (northwestern Barents Sea). Mar Ecol Prog Ser 118:199–213

Price NM, Harrison PJ (1987) Comparison of methods for the analysis of dissolved urea in seawater. Mar Biol 94: 307–317

Rasmussen H, Jørgensen BB (1992) Microelectrode studies of seasonal oxygen uptake in a coastal sediment: role of molecular diffusion. Mar Ecol Prog Ser 81:289–303

Revsbech NP (1989) An oxygen microelectrode with a guard cathode. Limnol Oceanogr 34:474–478

Revsbech NP, Jørgensen BB (1986) Microelectrodes and their use in microbial ecology. In: Marshall KC (ed) Advances in microbial ecology, Vol 9. Plenum Press, New York, p 293–352

Risgaard-Petersen N, Rysgaard S (1995) Nitrate reduction in sediments and waterlogged soil measured by ^{15}N techniques. In: Alef K, Nannipieri P (eds) Methods applied in soil and microbiology. Academic Press, London, p 287–295

Risgaard-Petersen N, Rysgaard S, Revsbech NP (1993) A sensitive assay for determination of $^{14}N/^{15}N$ isotope distribution in NO_3^-. J Microbiol Meth 17:155–164

Rosenfeld JK (1979) Ammonium adsorption in nearshore anoxic sediments. Limnol Oceanogr 24:356–364

Rysgaard S, Christensen PB, Nielsen LP (1995) Seasonal variation in nitrification and denitrification in estuarine sediment colonized by benthic microalgae and bioturbating infauna. Mar Ecol Prog Ser 126:111–121

Rysgaard S, Finster K, Dahlgaard H (1996) Primary production, nutrient dynamics and mineralization in a northeastern Greenland fjord during the summer thaw. Polar Biol 16:497–506

Rysgaard S, Thamdrup B, Risgaard-Petersen N, Fossing H, Berg P, Bondo PB, Dalsgaard T (1998) Seasonal carbon and nutrient mineralization in a high-Arctic coastal marine sediment, Young Sound, Northeast Greenland. Mar Ecol Prog Ser 175:261–276

Rysgaard S, Nielsen TG, Hansen BW (1999) Seasonal variation in nutrients, pelagic primary production and grazing in a high-Arctic coastal marine ecosystem, Young Sound, Northeast Greenland. Mar Ecol Prog Ser 179:13–25

Sambrotto RN, Goering JJ, McRoy CP (1984) Large yearly production of phytoplankton in the Western Bering Strait. Science 225:1147–1150

Schmid MK, Piepenburg D (1993) The benthos zonation of the

Disco Fjord, West Greenland. Medd Grønl 37:13–25
Sejr MK, Jensen KT, Rysgaard S (2000) Macrozoobenthic structure in a high-Arctic East Greenland fjord. Polar Biol 23:792–801
Stookey LL (1970) Ferrozine — a new spectrophotometric reagent for iron. Analyt Chem 42:779–781
Strickland JDH, Parsons TR (1972) A practical handbook of seawater analysis, 2nd edn. Bull Fish Res Board Can 167
Subbarao DV, Platt T (1984) Primary production of Arctic waters. Polar Biol 3:191–201
Thamdrup B (2000) Microbial manganese and iron reduction in aquatic sediments. Adv Microb Ecol 16:41–84
Thamdrup B, Canfield DE (1996) Pathways of carbon oxidation in continental margin sediments off central Chile. Limnol Oceanogr 41:1629–1650
Thamdrup B, Canfield DE, Ferdelman TG, Glud RN, Gundersen JK (1996) A biogeochemical survey of the anoxic basin Golfo Dulce, Costa Rica. Rev Biol Trop 44:19–33
Ullman WJ, Aller RC (1982) Diffusion coefficients in nearshore marine sediments. Limnol Oceanogr 27: 552–556
Wassmann P, Slagstad D (1993) Seasonal dynamics of particulate carbon flux in the Barents Sea. Polar Biol 13:363–372

Editorial responsibility: Otto Kinne (Editor), Oldendorf/Luhe, Germany

Submitted: February 24, 2000; Accepted: May 16, 2000
Proofs received from author(s): October 16, 2000